ACS OMEGA

http://pubs.acs.org/journal/acsodf

Article

Construction of a Drug Delivery System via pH-Responsive Polymeric Nanomicelles Containing Ferrocene for DOX Release and Enhancement of Therapeutic Effects

Chenggang Song, Fan Yang, Ruixuan Ji, Yin Lv,* and Zhong Wei*

Cite This: *ACS Omega* 2021, 6, 28242−28253

Read Online

ACCESS | Metrics & More | Article Recommendations

ABSTRACT: We report an amphiphilic block copolymer via poly(ethylene glycol) methyl ether-D_{labile}-poly(caprolactone)-ferrocene (mPEG-D_{labile}-PCL-Fc) to deliver anticancer drug doxorubicin (DOX). Lipase Novozyme-435 was used as a catalyst for ring-opening polymerization with ε-caprolactone, and an acid-sensitive Schiff base was used to connect the hydrophilic and hydrophobic parts; the ferrocene provided ferrous ions and was introduced at the end of the amphiphilic copolymer. The resulting copolymers were characterized by ^{1}H NMR/^{13}C NMR and could be self-assembled in an aqueous solution to form nanomicelles with PCL-Fc as a hydrophobic core and mPEG as a hydrophilic shell. Transmission electron microscopy showed that the micelles were spherical and nanosized before and after DOX loading. The blank micelles also showed good biocompatibility. The drug-loaded polymeric nanomicelles exhibited a positive anticancer effect relative to the copolymers without ferrocene; the therapeutic effect of drug-loaded micelles containing ferrocene was more obvious. In vitro drug release results also showed that the polymer had a good pH response. Confocal microscopy also showed that polymeric micelles can effectively deliver and release the drug; the polymer containing ferrocene also leads to significantly improved ROS levels in tumor cells. Ferrocene can effectively and synergistically inhibit tumor cells with DOX.

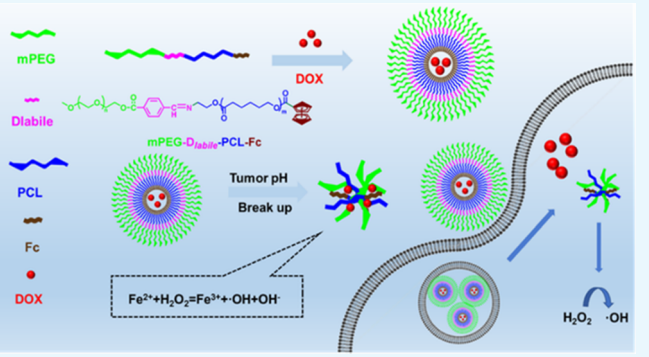

1. INTRODUCTION

Cancer remains one of the leading causes of death.[1−3] Chemotherapy remains one of the most commonly used methods for the treatment of cancer, but it has many side effects[4] and can have limited bioavailability. Therefore, improving the utilization rate and selectivity of drugs to cancer cells is essential for improving the effect of antitumor drugs. Here, a smart nanodrug delivery system can respond to different environmental stimuli and release drugs under specific conditions to achieve targeted and controlled release of drugs; this can reduce the toxic and side effects of drugs and reduce the damage of drugs to the human body. Therefore, to address the shortcomings of traditional treatments, it is necessary to develop an intelligent response nanodrug carrier system.

There are significant differences in the microenvironment between tumor cells and normal cells, and this difference can be used to design drug delivery systems with different response types to overcome these difficulties.[5] The tumor microenvironment (TME) has characteristics of hypoxia, microacid, enzyme overexpression (such as protease, phospoholipase, or glycosidase),[6] and high concentration of reactive oxygen.[7−10] The acidic microenvironment in tumor cells is the most obvious and most commonly used.[11−14] The pH of the extracellular environment of tumor cells is about 6.5, which is usually lower than that of normal tissue cells (pH 7.4); the pH of lysosomes is low (about 5.0−5.5). Based on these properties, scientists have developed various pH-sensitive drug carriers, including hydrazone bonds, aldehyde bonds, and imide bonds.

Programmed death is critical to disease research and normal development of the body.[15−17] Ferroptosis is a new type of programmed cell death proposed by Brent R. Stockwell in 2012. Ferroptosis depends on intracellular ferrous iron and is distinct from apoptosis as well as necrosis and autophagy in morphology, biochemistry, and genetics. In general, ferrous ions react with hydrogen peroxide in tumor cells to produce hydroxyl radicals to increase the oxidative stress of tumor cells. Research on ferroptosis caused by nanomedicine has only recently started, and most studies still use nanoiron to cause ferroptosis. However, there are some problems in the

Received: August 11, 2021
Accepted: September 30, 2021
Published: October 11, 2021

ACS Publications

© 2021 The Authors. Published by American Chemical Society

https://doi.org/10.1021/acsomega.1c04330
ACS Omega 2021, 6, 28242−28253

Scheme 1. Diagram of Self-Assembled DOX Drug-Loaded Polymeric Micelles, Drug Delivery, and pH-Responsive DOX Release

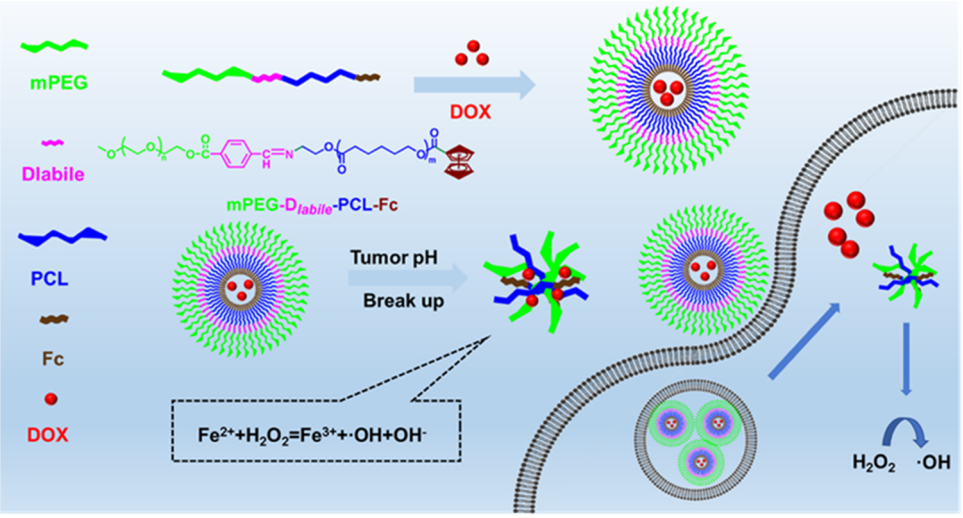

Scheme 2. Synthesis Route of the mPEG-D$_{labile}$-PCL-Fc Copolymer

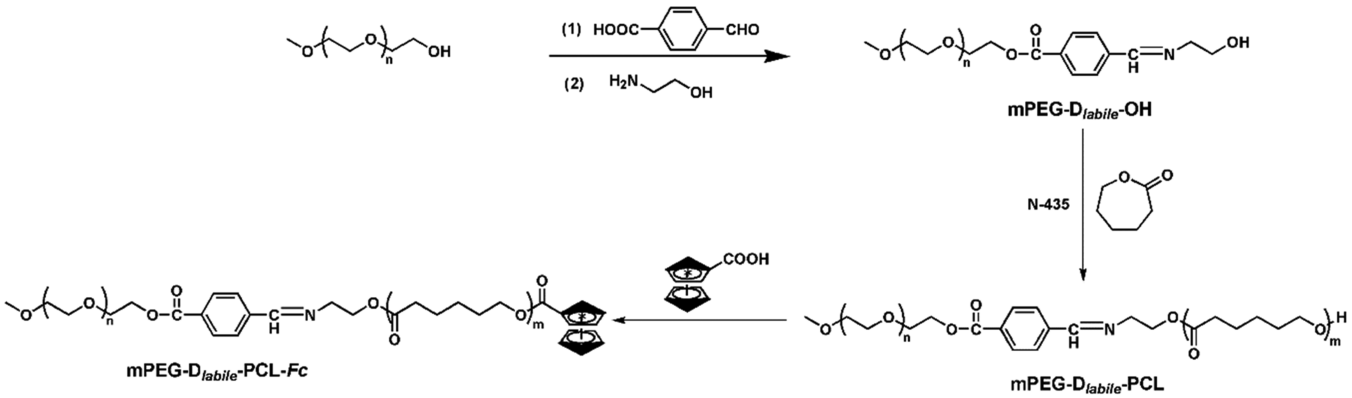

introduction of iron ions in the current research, which leads to the oxidation of ferrous ions in the transportation process, thus reducing the therapeutic effect. Crystalized iron releases slowly and is easily oxidized during transportation of ferrous ions. Therefore, avoiding oxidation and increasing the release rate has become a problem to be solved.[18−20] Ferrocene is a metal−organic complex composed of two cyclopentadienes and iron ions with good chemical stability, hydrophobicity, and nontoxicity. Ferrocene can be applied to the treatment of ferroptosis.[21−23] Amphiphilic copolymer micelles have a distinct core−shell structure with high biocompatibility, low cytotoxicity, high drug loading capacity, and good drug delivery efficiency. These micelles have excellent stability and high administration efficiency and can stabilize iron ions during the transportation process.

Here, we report pH-responsive self-assembled polymeric micelles with a Fenton-like reaction effect for efficient drug delivery and controlled release. This polymer micelle was formed by self-assembly of mPEG-D$_{labile}$-PCL-Fc and obtained by ring-opening polymerization. Hydrophilic PEG segments can form protective shells distributed outside the nanoparticles, providing a stable drug delivery system and prolonging the in vivo circulation time. Polycaprolactone provides hydrophobic segments. As a typical Fenton reagent, ferrocene contains two parallel cyclopentadiene rings giving ferrocene strong hydrophobicity. The electron transfer process of the ferrocene group to H_2O_2 has been proved in the Fenton-like reaction, and hydrophobic Fe $(Cp)^{2+}$ can be converted into hydrophilic Fe $(Cp)^{2+}$ during the reaction. It introduces ferrous ions in the Fenton reaction. The stability of the nanomicelles can ensure that ferrous iron is not oxidized during transportation. Scheme 1 shows that the pH-sensitive bond increases the environmental response of copolymer micelles and makes use of its mechanism of breaking under acidic conditions of tumor cells to promote the collapse of the polymer structure. This in turn releases antitumor drugs and ferrocene fragments. Based on this understanding, effective drug delivery and controlled release systems can be achieved (Scheme 2).

2. RESULTS AND DISCUSSION

2.1. Synthesis of the mPEG-D$_{labile}$-PCL-Fc Block Copolymer. We synthesized amphiphilic block copolymer mPEG-D$_{labile}$-PCL-Fc for the transportation of hydrophobic drug DOX.

Amphiphilic copolymer Polymer-1 (mPEG-*b*-PCL-OH) was synthesized by ring-opening polymerization of caprolactone with mPEG-OH as an initiator; Polymer-2 (mPEG-*b*-PCL-Fc) was synthesized by introducing ferrocene. Amphiphilic copolymer Polymer-3 (mPEG-D$_{labile}$-PCL) was synthesized by ring-opening polymerization of caprolactone with mPEG-D$_{labile}$-OH as an initiator, and Polymer-4 (mPEG-D$_{labile}$-PCL-Fc) was synthesized by introducing ferrocene. The polymer

https://doi.org/10.1021/acsomega.1c04330
ACS Omega 2021, 6, 28242−28253

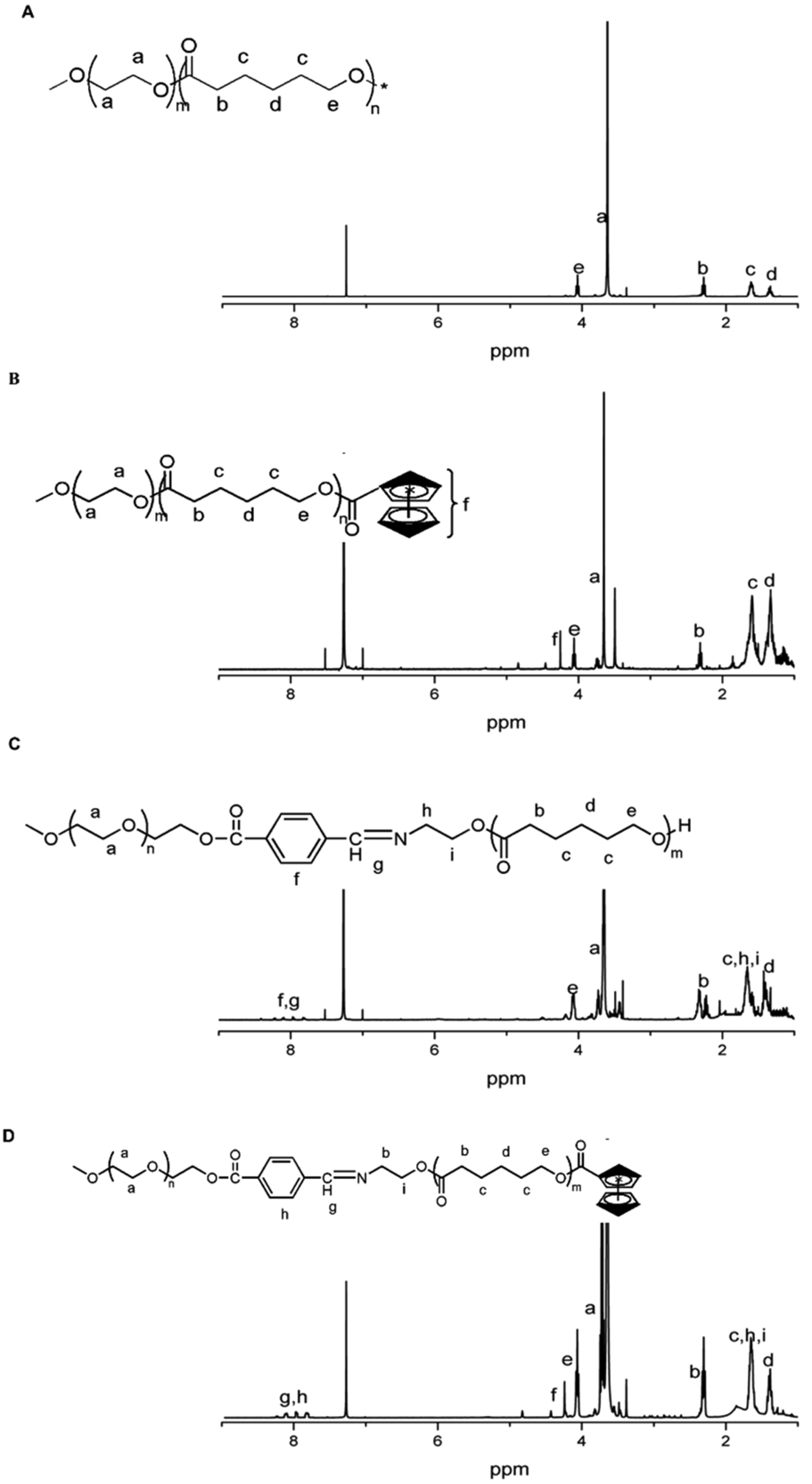

Figure 1. continued

https://doi.org/10.1021/acsomega.1c04330
ACS Omega 2021, 6, 28242−28253

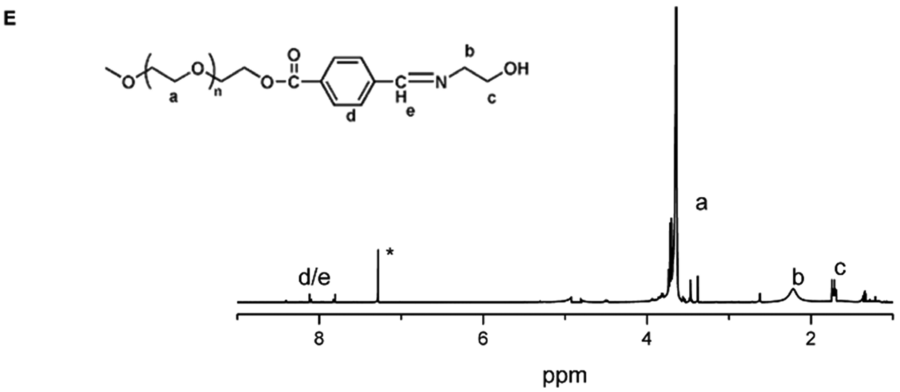

Figure 1. ^{1}H NMR (400MHz, $CDCl_3$) spectra of (A) (Polymer-1, mPEG-*b*-PCL-OH), (B) (Polymer-2, mPEG-*b*-PCL-Fc), (C) (Polymer-3, mPEG-D_{labile}-PCL), (D) (Polymer-4, mPEG-D_{labile}-PCL-Fc), and (E) (mPEG- D_{labile}-OH).

structures were confirmed by ^{1}H NMR. Figure 1A shows that the characteristic peak of the PEG fragment appears at about 3.65 ppm; 1.3−1.4, 1.6−1.7, 2.3−2.4, and 4.0−4.1 ppm are attributed to the characteristic peaks of $-OCH_2CH_2C\boldsymbol{H_2}CH_2$-$CH_2C(O)-$, $-OCH_2C\boldsymbol{H_2}CH_2C\boldsymbol{H_2}CH_2C(O)-$, $-OCH_2CH_2$-$CH_2CH_2C\boldsymbol{H_2}C(O)-$, and $-OC\boldsymbol{H_2}CH_2CH_2CH_2CH_2C(O)-$ on PCL, respectively. Figure 1E shows the characteristic peak of the Schiff base in the range of 7.8−8.2 ppm, which is consistent with the literature description,[24] indicating the successful synthesis of polymer. By integrating the characteristic peaks, the hydrophilic and hydrophobic ratio was 4.65:1, which is close to the feeding ratio of 5:1, indicating that the material was synthesized successfully. When Figure 1B is compared with Figure 1A, we see increased characteristic peaks at 4.12, 4.28, and 4.81 ppm due to ferrocene. In the 7.9−8.3 ppm characteristic peak (Figure 1C), the literature suggests a fragment for the benzene ring and the Schiff base. Finally, there is a characteristic peak of ferrocene, and the modification efficiency is about 40% of the peak in Figure 1C by integral calculation (Figure 1D).

As shown in Table 1, in the case of a PEG initiator, the resulting block copolymer was relevant to the monomer feed

Table 1. Characterization of Polymers

		^{1}H NMR[a]	molecular weight[b]		
		EG:CL:Fc	M_n	M_w	PDI
Polymer-1	mPEG-*b*-PCL-OH	4.65:1:0	6837	7534	1.10
Polymer-2	mPEG-*b*-PCL-Fc	4.65:1:0.02	7323	8353	1.14
Polymer-3	mPEG-D_{labile}-PCL	5.01:1:0	7363	8229	1.12
Polymer-4	mPEG-D_{labile}-PCL-Fc	5.01:1:0.02	7646	8434	1.11

[a]Calculated by ^{1}H NMR. [b]Measured by GPC.

ratio. Furthermore, the molecular weights (M_n) of Polymer-1 to Polymer-4 were 6837, 7323, 7376, and 7646 g/mol and their PDI values were 1.10, 1.14, 1.12, and 1.11, respectively, which were measured by gel permeation chromatography (GPC) analysis. The results of their PDI values showed narrow molecular weight distributions.

The polymer structures were confirmed by ^{13}C NMR. Figure 2A shows that the characteristic peak of the PEG fragment appears at about 71 ppm; 19.8, 28.4, 34.2, 39.8, and 59.6 ppm are attributed to the characteristic peaks of $-CH_2\boldsymbol{C}H_2CH_2CH2C(O)-$, $-CH_2CH_2\boldsymbol{C}H_2CH_2C(O)-$, $-CH_2CH_2CH_2\boldsymbol{C}H_2C(O)-$, and $-\boldsymbol{C}H_2CH_2CH_2CH_2C(O)-$ on and $-CH_2CH_2CH_2CH_2\boldsymbol{C}(O)-$ on PCL, which is consistent with the literature description,[25−27] indicating the successful synthesis of the polymer. Compared with Figure 2A, Figure 2B shows the characteristic peaks at 26.8 and 30 ppm, indicating the successful introduction of ferrocene. Compared with Figure 2B, Figure 22C shows the characteristic peaks of the benzene ring at 130 and 140 ppm, indicating the successful introduction of the Schiff base. Compared with Figure 2C,2 Figure 2D shows the characteristic peaks at 26.8 and 30 ppm, indicating the successful introduction of ferrocene. This indicated the successful synthesis of mPEG-D_{labile}-PCL-Fc.

2.2. Characterization of the Polymeric Micelles. The polymeric micelles were prepared by a dialysis method. The synthesized polymers can form polymer micelles with mPEG as a shell and PCL as a core in an aqueous solution.

Pyrene is a fluorescent substance with strong hydrophobicity. In the aqueous phase, it will preferentially enter the hydrophobic core of the micelles upon formation of micelles. The fluorescence intensity changes sharply from weak to strong when pyrene is wrapped in micelles. It is widely used to detect the formation of micelles. In this paper, pyrene was used as a hydrophobic fluorescent probe to study the micellar behavior of mPEG-$PCL_{5:1}$ (Polymer-1), mPEG-$PCL_{5:1}$-Fc (Polymer-2), mPEG-D_{labile}-$PCL_{5:1}$ (Polymer-3), and mPEG-D_{labile}-$PCL_{5:1}$-Fc (Polymer-4) in an aqueous solution. When the concentration of the amphiphilic copolymer in water is greater than its critical micelle concentration (CMC), the micelle structure with a hydrophobic segment as the core and a hydrophilic segment as the shell can be formed and can be stably dispersed in water.[28] Table 2 shows that the CMC values of Polymer-1, Polymer-2, Polymer-3, and Polymer-4 were 2.3, 2.5, 2.4, and 2.8 mg/L, respectively. Several polymers have basically the same hydrophilic and hydrophobic ratios, and their CMC is also relatively close, thus leading to smaller CMC values. They also have a stable micelle structure.[29]

Dynamic light scattering (DLS) and transmission electron microscopy (TEM) were used to characterize the size and distribution of the resulting polymeric micelles. Table 2 lists the hydrated particle sizes of the prepared block copolymers with different structures measured by DLS. Table 2 shows that the average hydration particle sizes of Polymer-1, Polymer-2, Polymer-3, and Polymer-4 were 143.9, 169.7, 145.8, and 159.9 nm, respectively. The particle size of Polymer-2 is larger than Polymer-1, which may be due to the increase in hydrophobic segments upon the addition of ferrocene.[30] Under the condition of constant hydrophilic segments, the

https://doi.org/10.1021/acsomega.1c04330
ACS Omega 2021, 6, 28242−28253

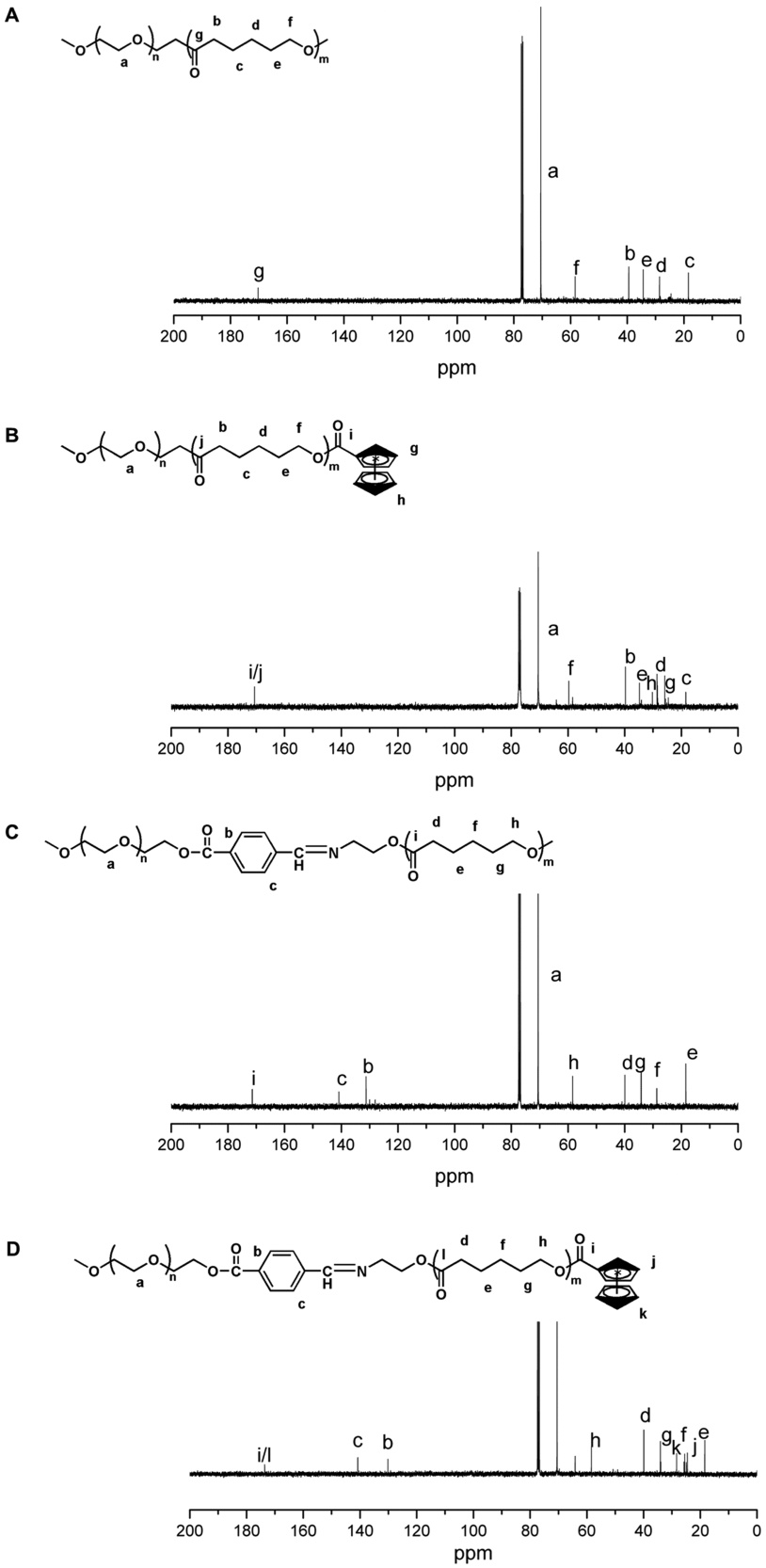

Figure 2. ^{13}C NMR (400MHz, $CDCl_3$) spectra of (A) (Polymer-1, mPEG-*b*-PCL-OH), (B) (Polymer-2, mPEG-*b*-PCL-Fc), (C) (Polymer-3, mPEG-D_{labile}-PCL), and (D) (Polymer-4, mPEG-D_{labile}-PCL-Fc).

core of the micelles increases and the particle size increases. The particle size of Polymer-4 is also larger than that of Polymer-3, which is probably due to the same reason.

2.3. DOX Loading. The potential of the polymer carrier was evaluated using anticancer drug DOX as a model. The mass ratio of the copolymer to doxorubicin was 10:1, and

https://doi.org/10.1021/acsomega.1c04330
ACS Omega 2021, 6, 28242−28253

Table 2. Properties of Blank/DOX-Loaded Copolymer Micelles

		diameter (nm)					
	CMC (mg/L)	by DLS[a]	by TEM[b]	PDI by DLS[c]	DLC (wt %)[d]	EE (wt %)[d]	Fc (mg/g)[e]
Polymer-1	2.3	143.9/120.5	43.5/24.8	0.135/0.210	6.1	67.1	
Polymer-2	2.5	169.7/134.7	55.7/44.4	0.124/0.188	6.8	74.8	7.8
Polymer-3	2.4	145.8/110.8	46.9/34.5	0.141/0.301	7.1	78.1	
Polymer-4	2.8	159.9/130.0	48.6/34.5	0.117/0.258	8.0	88.2	8.2

[a]Hydrodynamic diameter of blank micelles/DOX-loaded micelles in water. [b]Estimated by TEM. [c]Polvdispersity index of blank micelles/DOX-loaded micelles obtained from DLS measurements. [d]Measured by a UV spectrophotometer at 482 nm. [e]Measured by a UV spectrophotometer at 447 nm.

hydrophobic anticancer drug DOX was encapsulated in amphiphilic polymer micelles by dialysis. The drug loading and encapsulation efficiency of the copolymers are shown in Table 2. Polymer-2 and Polymer-4 have higher encapsulation efficiency and drug loading than Polymer-1 and Polymer-3, which may be due to their longer hydrophobic chain, thus resulting in a larger hydrophobic cavity and more drug loading. In addition, Table 2 also shows that ferrocene has a high introduction rate, which is basically about 8.0 mg/g (Figure 3).

Table 1 shows that the particle size of the polymer micelles after drug loading has been reduced to different degrees. This may be due to the hydrophobic drug entering the micelle core, which causes the hydrophobic core to shrink and the particle size to decrease.[31] In addition, the TEM results show that the polymers before and after drug loading are spherical, and the particle size is less than the hydrated particle size; the size trend is almost the same as the hydrated particle size.

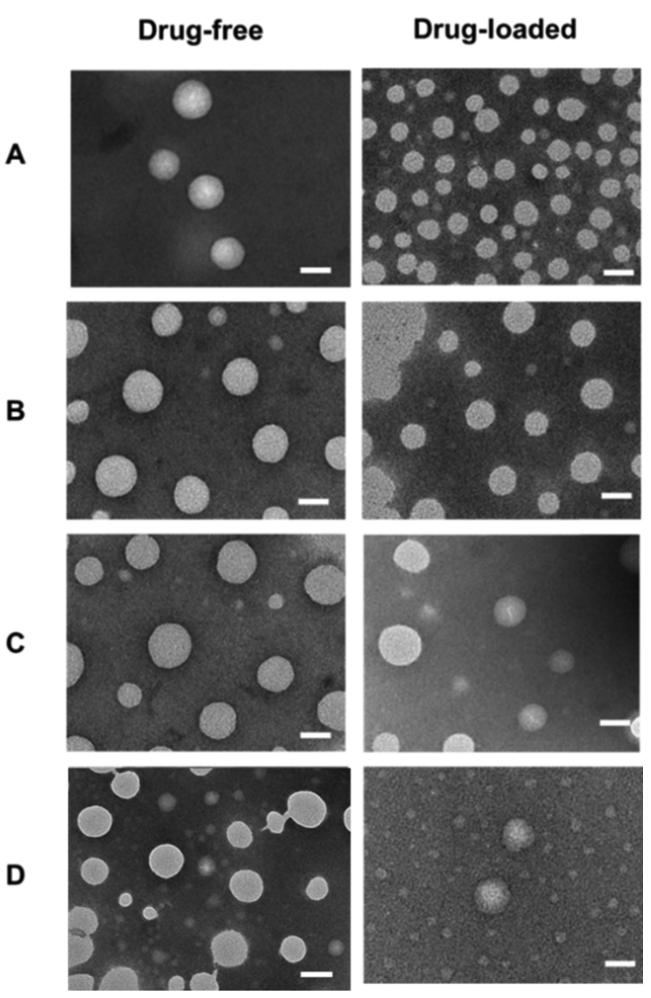

Figure 3. Transmission electron microscopy images of drug-free and drug-loaded polymeric micelles based on Polymer-1 (A), Polymer-2 (B), Polymer-3 (C), and Polymer-4 (D). Scale bar: 50 nm.

2.4. In Vitro and Intercellular Drug Release. We used hydrophobic anticancer drug DOX as a model to study the in vitro release behavior of amphiphilic copolymer micelles.

Polymer-1, Polymer-2, Polymer-3, and Polymer-4 DOX-loaded micelles were placed in a dialysis bag and dissolved in buffer solutions of pH 7.4, 6.5, and 5.0, respectively. The dialysis solution was taken at different times, and the fluorescence intensity of the solution at 555 nm was tested. The cumulative release amount of the polymer was calculated, and the curve was plotted. Figure 4 shows that the cumulative drug release of the four polymers was about 35% at pH 7.4 within 48 h. The drug release rate increased as the pH value decreased. The drug release rate in Figure 4C,4D increased more obviously than that in Figure 4A,4B. The cumulative drug release of Figure 4C,4D was about 60% at pH 6.5 within 48 h, and it increased to 80% at pH 5.0. This may be due to the presence of acid-sensitive Schiff bases in Polymer-3 and Polymer-4 compared to Polymer-1 and Polymer-2. Polymer-3 and Polymer-4 contain acid-sensitive Schiff bases compared with Polymer-1 and Polymer-2, and Schiff bases will break under acidic conditions; thus, the micelle structure will collapse, accelerating the release of DOX. This is consistent with the literature, which indicates that Polymer-3 and Polymer-4 have acid-sensitive responses.[32]

From Figure 5, we can see that the particle size of Polymer-4 increases in varying degrees within 48 h under the condition of phosphate-buffered saline (PBS) 7.4, which is caused by the expansion of micelles in water, while under the condition of ABS 5.0, the particle size of Polymer-4 changes significantly, which is caused by the fracture of the Schiff base under acidic conditions.[33]

From Figure 6, it can be seen that the particle size of drug-loaded Polymer-1 and Polymer-2 after drug release in the pH 5.0 solutions at 37 °C has obviously increased and even agglomeration occurs, which is caused by the release of the drug by the polymer, resulting in the reduction of internal attraction. However, the drug-loaded micelle structure of Polymer-3 and Polymer-4 containing acid-sensitive bond basically collapses in the same condition, which is caused by the release of the drug by polymer fracture in an acidic environment.

2.5. In Vitro Cytotoxicity. Biodegradable polyesters have low toxicity and good biocompatibility, and polyethylene glycol is also an FDA-approved polymer. The cytotoxicity of micelles was detected by the 3-(4,5-dimethylthiazol-2-yl)-2,5-diphenyl-2H-tetrazolium bromide (MTT) assay. Figure 7A shows that the cell survival rates were basically above 90% when the blank micelles with different concentrations were cocultured with

https://doi.org/10.1021/acsomega.1c04330
ACS Omega 2021, 6, 28242−28253

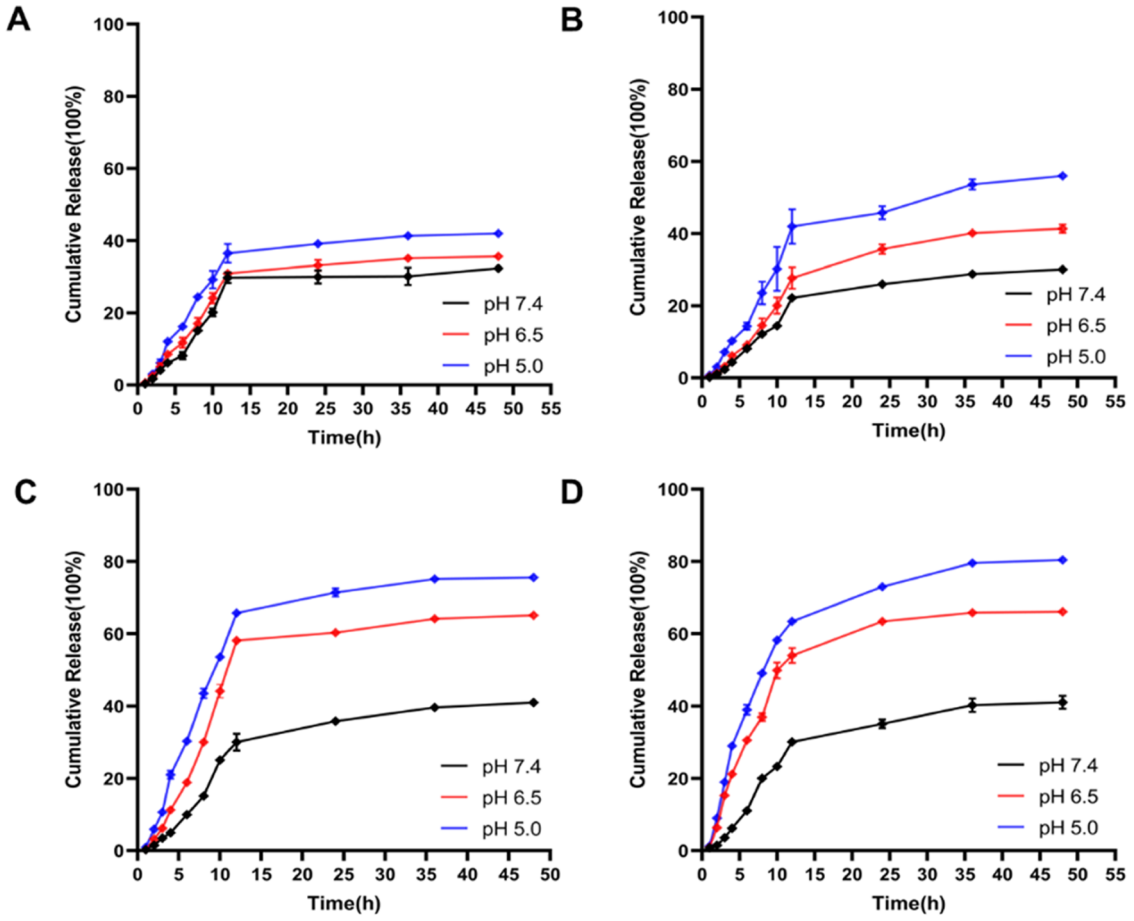

Figure 4. In vitro drug release profiles from DOX-loaded micelles based on Polymer-1 ((A), mPEG-*b*-PCL), Polymer-2 ((B), mPEG-*b*-PCL-Fc), Polymer-3 ((C), mPEG-D_{labile}-PCL), and Polymer-4 ((D), mPEG-D_{labile}-PCL-Fc) in pH 7.4, 6.5, and 5.0 solutions at 37 °C, respectively.

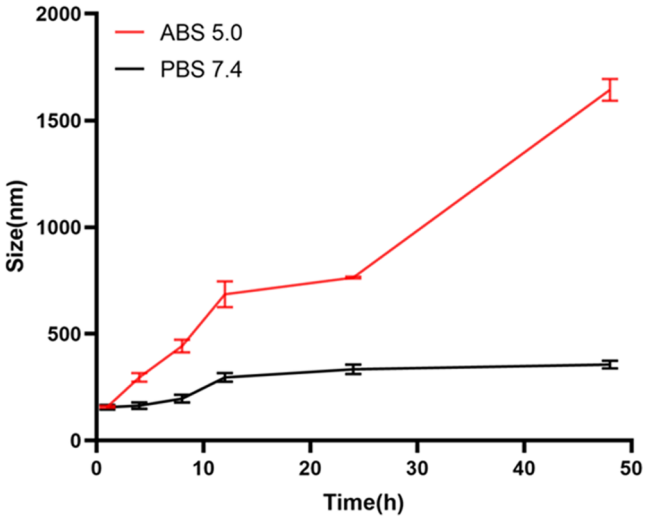

Figure 5. Size changes of Polymer-4 in different conditions.

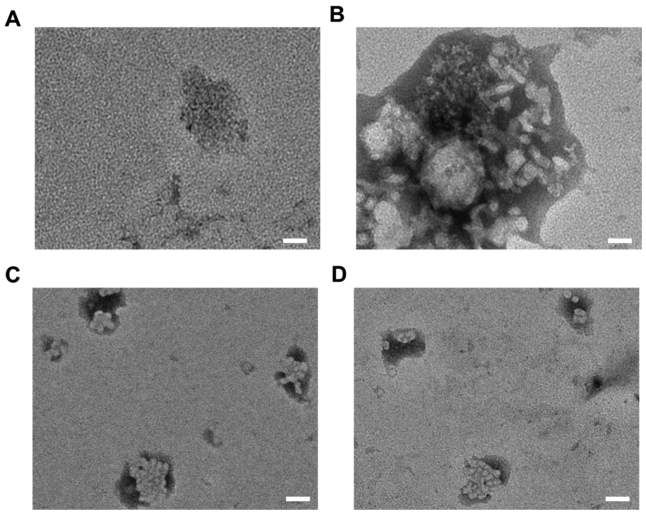

Figure 6. TEM images of drug-loaded Polymer-1 (A), Polymer-2 (B), Polymer-3 (C), and Polymer-4 (D) after drug release (pH 5.0 solutions at 37 °C). Scale bar: 50 nm.

COS7 cells for 48 h. The results show that the polymer had low cytotoxicity and good frontal biocompatibility.

The effects of drug-loaded polymer micelles and DOX concentration on 4T1 tumor cells are shown in Figure 7B. The inhibitory effect was the most obvious at 10 μg/mL. Polymer-2 with ferrocene has a better inhibitory effect on 4T1 cells than Polymer-1 without ferrocene, which indicates that the iron death caused by ferrocene can better inhibit cells. Polymer-3 containing a pH-responsive also had better inhibitory effects against 4T1 cells. In addition, Polymer-4 has sensitive bonds, and ferrocene has the best effect. This may be because of faster drug release of the responsive polymer; the polymer without a sensitive bond has a delay in drug release, and the ferrous ion in ferrocene can increase the inhibitory effect of drugs on tumors

https://doi.org/10.1021/acsomega.1c04330
ACS Omega 2021, 6, 28242−28253

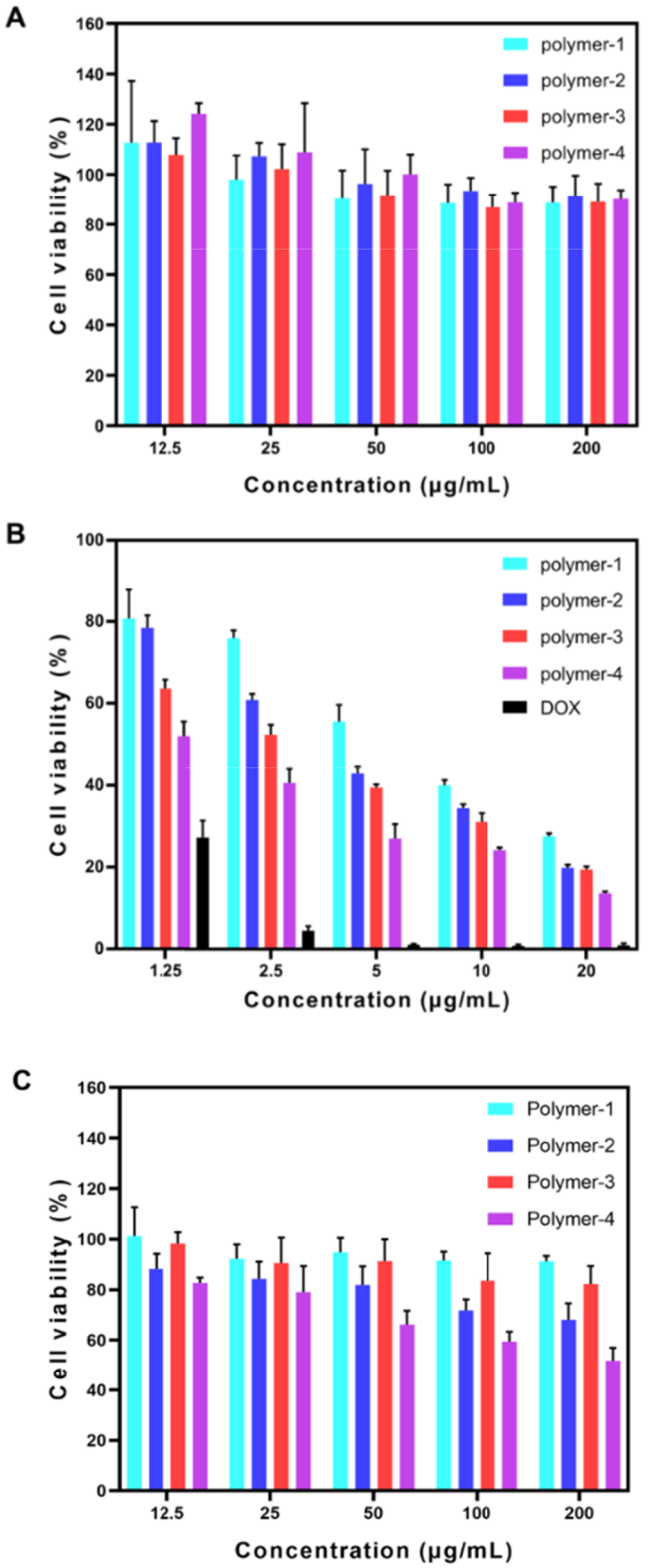

Figure 7. Cytotoxicity of drug-free polymeric micelles in COS7 cells (A), DOX-loaded polymeric micelles in 4T1 cells (B), and drug-free polymeric micelles in 4T1 cells (C) shown as mean ± standard deviation (SD) (n = 5).

due to its Fenton reaction. Ferrocene can synergistically inhibit tumor cells by DOX. As shown in Figure 7C, Polymer-1 and Polymer-3 without ferrocene have little effect on the viability of 4T1 cells, Polymer-2 and Polymer-4 containing ferrocene inhibited the activity of 4T1 cells significantly, and Polymer-4 containing acid-sensitive groups and ferrocene had the best inhibitory effect, which also fully proved the inhibitory effect of ferrocene on cell activity. At the highest concentration tested (10 μg/mL), free DOX and DOX-loaded Polymer-4 both exhibited lower cell viability (below 18%). The IC50 values of free DOX were 0.85 μg/mL; it did show lower cancer cell survival. Moreover, Polymer-4 exhibited obviously higher cytotoxicity than copolymers without ferrocene or the acid-sensitive copolymers (Polymer-1, Polymer-2, and Polymer-3), while similar results have also been reported in the other cancer cells.[26] The IC50 values of Polymer-1, Polymer-2, Polymer-3, and Polymer-4 were determined to be 7.14, 4.53, 3.80, and 1.85 μg/mL, respectively, for 4T1 cells. Meanwhile, as shown in Figure 8, cells, laser confocal microscopy (CLSM) studies revealed a much more amount of DOX internalized by Polymer-4 than that by the polymer without ferrocene or the acid-sensitive copolymers (Polymer-1, Polymer-2, and Polymer-3).

2.6. Cellular Uptake. To investigate how drugs enter cells and their distribution in cells, laser confocal microscopy (CLSM) was used to observe the endocytosis of drug-loaded micelles with Polymer-1, Polymer-2, Polymer-3, and Polymer-4. The 4T1 cells were cocultured with drug-loaded micelles for 4 and 12 h, and the nucleus was labeled with Hoechst 33342 with blue fluorescence. Adriamycin showed red fluorescence. The results are shown in Figure 8. As the culture time increases from 4 to 12 h, free DOX and drug-loaded polymer micelles 1/2/3/4 can enter the cells and gradually distribute in the cytoplasm and nucleus.

Figure 8I,J shows that most of the DOX entered the cells after 4 h of DOX treatment, and a small amount of DOX was enriched in the nucleus. After 12 h of coculture, much amount of DOX was enriched in the nucleus because DOX could enter the cells and rapidly diffuse and enrich into the nucleus.[34] Figure 8A,8B shows that the red fluorescence of DOX was concentrated in the nucleus and cytoplasm after 4 h of cell culture of drug-loaded micelle Polymer-1 and 4T1 cells. This was even more obvious after 12 h. Figure 8C,8D is similar to Figure 8A,B. Figure 8E,8F shows that the red fluorescence of DOX was distributed in the cytoplasm and nucleus after 4 h of drug-loaded micelle Polymer-3 and 4T1 cell culture. After 12 h, the red fluorescence was more obvious and was related to the rapid drug release rate of Polymer-3. Figure 8G,8H shows that the red fluorescence of DOX was concentrated in the nucleus and cytoplasm after 4 h of cell culture of drug-loaded micelle Polymer-1 and 4T1. After 12 h, the red fluorescence was more obvious, which may be due to the acid-sensitive structure of drug-loaded micelle Polymer-4 and the rapid drug release rate. Polymer micelles can effectively transfer and release DOX.

2.7. ROS Level. We tested ROS levels using 2,7-dichlorodihydrofluorescein diacetate (DCFH-DA). DCFH-DA itself has no fluorescence and is oxidized to DCF by ROS after entering cells, resulting in green fluorescence. In Figure 9, we can see that Polymer-1 and Polymer-3 have relatively weak fluorescence intensity. The fluorescence intensity of Polymer-2 and Polymer-4 was significantly stronger than that of Polymer-1 and Polymer-3, indicating that the ROS level of tumor cells treated with Polymer-2 and Polymer-4 was significantly increased—this may be due to the Fenton reaction of ferrous ions in ferrocene, producing hydroxyl radicals and increasing the ROS levels in vivo. Figure 9 shows that the fluorescence intensity of Polymer-4 is stronger than that of Polymer-2, which may be because Polymer-4 contains acid-sensitive bonds and

https://doi.org/10.1021/acsomega.1c04330
ACS Omega 2021, 6, 28242−28253

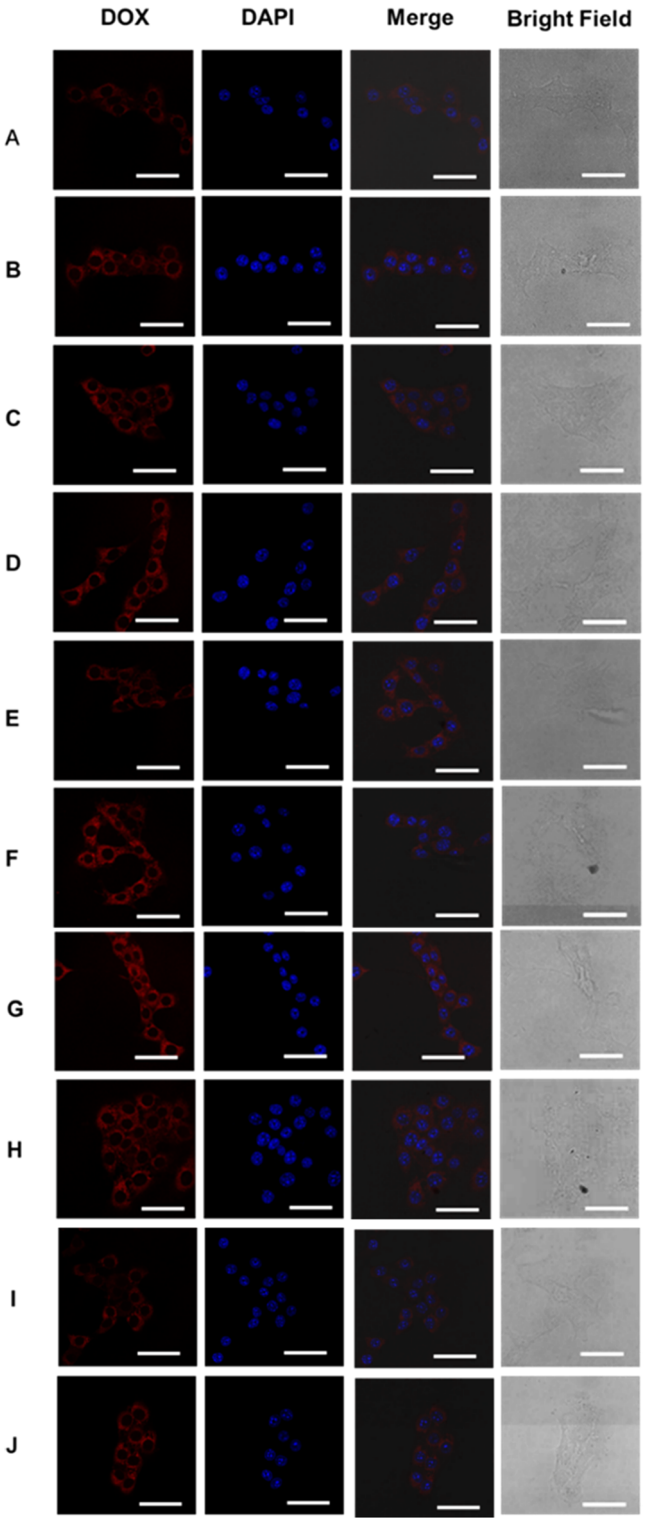

Figure 8. At the same concentration of DOX (5.0 mg/L), 4T1 cells were incubated with DOX-loaded micelles based on Polymer-1 (A, B), Polymer-2 (C, D), Polymer-3 (E, F), Polymer-4 (G, H), and free DOX (I, J) for 4 h (A, C, E, G, I) and for 12 h (B, D, F, H, J). Scale bar: 50 nm. For each panel, images from the left to right show only DOX fluorescence, nuclear staining by Hoechst 33342, overlays of cells with DOX fluorescence, and nuclear staining by Hoechst 33342, and bright field.

the release of ferrocene is fast. This is because hydrophobic Fe $(Cp)^{2+}$ can be converted into hydrophilic Fe $(Cp)^{2+}$ during the reaction. It introduces ferrous ions in the Fenton reaction.[35] These results suggest that ferrocene can effectively enhance ROS levels in vivo.

3. CONCLUSIONS

Amphiphilic block copolymers mPEG-D_{labile}-PCL-Fc were successfully synthesized by enzymatic ring-opening polymerization. The CMC, micelle size, drug loading, and encapsulation rate of DOX-loaded micelles; DOX release behavior; and anticancer effect are closely related to the polymer structure. Polymers containing sensitive bonds have a faster release rate. Polymers can effectively deliver and release drugs. Ferrocene-containing polymers have high drug loading and cytotoxicity, and they can promote cells to produce a large number of ROS. The Fenton reaction of ferrocene can assist drugs in inhibiting tumor cells.

4. EXPERIMENTAL SECTION

4.1. Materials. Poly(ethylene glycol) methyl ether (mPEG, MWN-5000), *N,N′*-dicyclohexylcarbodiimide (DCC), 4-dimethylaminopyridine (DMAP), pyrene (>99%), 4-carboxybenzaldehyde (FA), ethanolamine, ε-caprolactone (CL), ferrocenecarboxylic acid (Fc, 98%) and pyrene (97%), and 2,7-dichlorodihydrofluorescein diacetate (DCFH-DA), all of the above drugs, were purchased from Aladdin, with purity ≥99% unless specified. Novozyme-435 (immobilized Candida antarctica lipase B on methacrylate macroporous resin) was purchased from Sigma-Aldrich. *N,N*-Dimethylformamide (DMF), dichloromethane (DCM), tetrahydrofuran (THF), and dimethyl sulfoxide (DMSO), the above solvents, were dried before use and were from Tianjin Fuyu Fine Chemical Co., Ltd. DOX hydrochloride (DOX) was from Dalian Meilun Biology Technology Co. Ltd. (China).

4.2. Synthesis of the mPEG-D_{labile}-PCL-Fc block Copolymer. *4.2.1. Synthesis of mPEG-D_{labile}-OH.*[36] mPEG (MWN-5000, 2 g, 0.4 mmol), DCC (0.8253 g, 4 mmol), and DMAP (0.1222 g, 1 mmol) were stirred in dehydrated dichloromethane at room temperature until completely dissolved. *p*-Formyl benzoic acid (1.2 g, 8 mmol) was added and stirred at room temperature for 24 h. The resulting solution was filtered and concentrated, precipitated with isopropanol, then filtered, and dried to obtain mPEG-CHO. The obtained mPEG-CHO (l g, 0.19 mmol) and aminoethanol (0.015 g, 0.24 mmol) were dissolved in DMSO. After stirring for 4 h at 40 °C, the concentrated solution was precipitated with n-hexane and dried in vacuum for 48 h to obtain mPEG-D_{labile}-OH.

4.2.2. Synthesis of mPEG-D_{labile}-PCL. mPEG-D_{labile}-OH (0.5 g, 0.096 mmol), ε-CL (0.25 g, 2.17 mmol), and Novozyme-435 (10 wt % with monomer weight) were dissolved in toluene and stirred at 70 °C for 4 h. Then, the filtrate was concentrated and dissolved in dichloromethane, dialyzed (MWCO: 3500 Da) for 48 h in distilled water, and refreshed every 4 h. The resulting solution was lyophilized to obtain mPEG-D_{labile}-PCL (denoted Polymer-3). At the same time, mPEG-*b*-PCL without the Schiff base structure was synthesized as a comparison sample according to the literature,[14] denoted Polymer-1.

4.2.3. Synthesis of mPEG-D_{labile}-PCL-Fc. mPEG-D_{labile}-PCL-OH (0.2 g, 0.025 mmol), DCC (0.054 g, 0.25 mmol), and DMAP (0.008 g, 0.065 mmol) were dissolved in DMF at room temperature. After complete dissolution, ferrocene acid (Fc) was added and stirred at room temperature for 48 h. The obtained solution is filtered, concentrated, and then placed in a

https://doi.org/10.1021/acsomega.1c04330
ACS Omega 2021, 6, 28242−28253

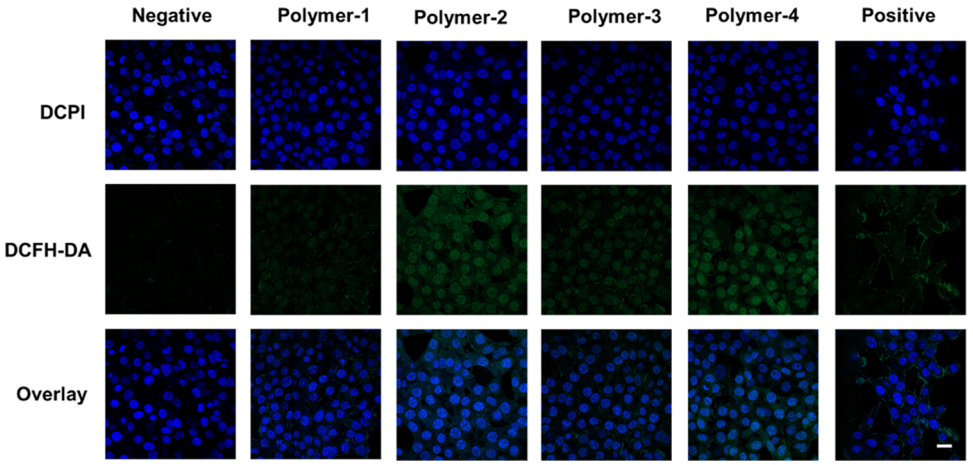

Figure 9. ROS levels of micelles Polymer-1/Polymer-2/Polymer-3/Polymer-4 cultured with 4T1 cells for 24 h. Scale bar: 30 nm.

dialysis bag (MWCO 3500 Da). After dialysis in 2000 mL of distilled water for 48 h, the water was altered every 4 h. The resulting solution was lyophilized to obtain mPEG-D_{labile}-PCL-Fc (denoted Polymer-4). According to Polymer-1, mPEG-*b*-PCL-Fc (denoted Polymer-2) without the Schiff base but containing ferrocene was synthesized as a contrast sample.

4.3. Physicochemical Characterization. ^{1}H NMR and ^{13}C NMR spectra were performed on a nuclear magnetic resonance spectrometer (ADVANCE 400, Bruker, Germany) using tetramethylsilane (TMS) as an internal reference and $CDCl_3$ as the solvent. Fluorescence spectra were recorded using an F-4700 (HITACHI) spectrofluorometer (slit widths, 5 nm). An electron microscope was used for transmission electron microscopy (TEM, HT7700, Hitachi, Japan) observation at 200 kV accelerating voltage. The liquid was dropped (0.1 mg/mL) onto a Formvar thin-film copper grid and dried. A Micromeritics Instrument (Nano-PLUS-3, Otsuka Technology Co., Ltd., Japan) was used to measure the size distribution of the micelle solution. Before measurements, the micelle solution (0.1 mg/mL) was passed through 0.45 μm aperture syringe filters. The test was conducted at room temperature three times to determine the average. The number-average molecular weight and polydispersity of copolymers were determined by gel permeation chromatography (GPC) equipped with a Waters high-performance liquid chromatography (HPLC) system.

4.4. Preparation of DOX-Loaded and Blank Polymeric Micelles. The DOX-loaded and blank micelles were prepared by the dialysis method as reported. In short, the polymer (60 mg), DOX·HCl (6 mg), and triethylamine (TEA, 60 μL) were dissolved in 6 mL of DMF and stirred in the dark for 2 h at room temperature. The solutions were transferred into a dialysis tube (MWCO: 3500 Da) and dialyzed against distilled water for 24 h. The distilled water was refreshed every 4 h. The obtained solutions were then filtered and lyophilized.

A certain amount of freeze-dried drug-loaded copolymer micelles was dissolved in DMF, and the UV absorbance was measured at 482 nm. The UV−vis wavelength of blank micelles was 447 nm. The drug loading content (DLC) and entrapment efficiency (EE) were calculated according to the following formula

$$\text{drug loading content (wt \%)} = \frac{\text{weight of drug in micelles}}{\text{weight of drug} - \text{loaded micelles}} \times 100$$

$$\text{entrapment efficiency (wt \%)} = \frac{\text{weight of drug in micelles}}{\text{weight of drug fed initially}} \times 100$$

$$\text{Fc(mg/g)} = \frac{\text{weight of Fc}}{\text{weight of blank micelles}}$$

4.5. In Vitro Release of Drug-Loaded Micelles. The drug release behavior of DOX in drug-loaded micelles was studied at 37 °C in pH 7.4, 6.5, and 5.0 buffer solutions. A certain amount of freeze-dried drug-loaded micelles was dissolved in 3 mL of buffer solutions with different pH values, and the dialysis bag (MWCO 3500 Da) was added to the corresponding 25 mL of buffer solution. The solution was placed in a shaker at 110 rpm and 37 °C; 3 mL of external solution was added at intervals. The fluorescence intensity was measured at 482 nm excitation wavelength. The cumulative release of drugs was calculated according to the formula by labeling curve

$$\text{cumulative release (\%)} = \frac{V_e \sum_1^{n-1} C_i + V_0 C_n}{m} \times 100$$

where V_e is the volume of the solution taken out each time, V_0 is the total volume of the external solution, C_i is the concentration of DOX in the solution taken out at time, m is the mass of DOX in the drug-loaded micelles in the dialysis bag, and n is the sampling time.

4.6. In Vitro Cytotoxicity Assay. The MTT method was used to evaluate the toxicity of free DOX, copolymer micelles, and drug-loaded micelles on COS7 cells (African Green Monkey Kidney Cells) and 4T1 cells (mouse breast cancer cell). The cells were seeded in a 96-well plate at a density of 6000 cells/well; 100 μL of Dulbecco's modified Eagle's medium (DMEM) was added, and the solution was cultured for 24 h in an incubator containing 5% CO_2 at 37 °C. Different concentrations of sample solution (100 μL) were added, continued to culture 48 h after adding 20 μL of MTT solution (5 mg/mL), recultured for 4 h; finally, all of the medium and MTT was sucked out, 150 μL of DMSO was added to each hole, and the absorbance of each hole at 570 nm was detected by an enzyme-labeled instrument. The cell survival rate was calculated according to the following formula

https://doi.org/10.1021/acsomega.1c04330
ACS Omega 2021, 6, 28242−28253

$$\text{relative cell viability}(\%) = \frac{A_{\text{ample}} - A_0}{A_{\text{control}} - A_0} \times 100$$

where A_0 is the blank absorbance value, A_{control} is the absorbance value of the control group, and A_{sample} is the absorbance value of the material. The absorbance value (A) is based on the average values of three independent parallel samples, and the results are expressed as mean ± standard deviation (SD).

4.7. Cellular Uptake. The uptake of drug-loaded micelles by 4T1 cells was observed by laser confocal microscopy (CLSM), with free DOX as the control. 4T1 cells (1×10^5 cells/well) were seeded in 25 mm dishes and cultured in a 5% CO_2 incubator at 37 °C for 24 h. A certain concentration of drug-loaded micelles and free DOX solution was added to the culture dish and then cultured in the incubator for 4 and 24 h, respectively. The medium was sucked out, and the cells were fully washed with PBS; the nuclei were stained with 10 μL of Hoechst 33342 (2 μg/μL); after 15 min, the cells were washed three times with PBS again. Finally, 1 mL of DMEM was added. The fluorescence signals of DOX and Hoechst 33342 were excited at 488 and 405 nm, respectively.

4.8. ROS Level Test. The 4TI cells were inoculated in a glass culture dish at 1×10^5 cells/well and cultured overnight in 2 mL of DMEM medium containing 10% fetal bovine serum (FBS) at 37 °C. The medium was replaced with fresh FBS containing DMEM, and drug-loaded polymers were added. After 24 h of culture, the medium was replaced with fresh DMEM (2 mL) containing DCFH-DA (10 μM). After 30 min of culture, the cells were washed with cold PBS three times, and the fluorescence of DCFH-DA (Ex, 488 nm; Em, 500−540 nm) decomposed under light stimulation was observed by laser scanning confocal microscopy (CLSM).

AUTHOR INFORMATION

Corresponding Authors

Yin Lv − *School of Chemistry and Chemical Engineering/Key Laboratory for Green Processing of Chemical Engineering of Xinjiang Bingtuan, Shihezi University, Shihezi, Xinjiang 832003, China*; Email: ag_125@163.com

Zhong Wei − *School of Chemistry and Chemical Engineering/Key Laboratory for Green Processing of Chemical Engineering of Xinjiang Bingtuan, Shihezi University, Shihezi, Xinjiang 832003, China*; orcid.org/0000-0002-1653-4838; Email: steven_weiz@sina.com

Authors

Chenggang Song − *School of Chemistry and Chemical Engineering/Key Laboratory for Green Processing of Chemical Engineering of Xinjiang Bingtuan, Shihezi University, Shihezi, Xinjiang 832003, China*

Fan Yang − *School of Chemistry and Chemical Engineering/Key Laboratory for Green Processing of Chemical Engineering of Xinjiang Bingtuan, Shihezi University, Shihezi, Xinjiang 832003, China*

Ruixuan Ji − *School of Chemistry and Chemical Engineering/Key Laboratory for Green Processing of Chemical Engineering of Xinjiang Bingtuan, Shihezi University, Shihezi, Xinjiang 832003, China*

Complete contact information is available at: https://pubs.acs.org/10.1021/acsomega.1c04330

Notes

The authors declare no competing financial interest.

ACKNOWLEDGMENTS

The authors gratefully acknowledge financial support from the Program for Young Innovative Talents of Shihezi University (No. CXRC201704).

REFERENCES

(1) Duncan, R.; Ringsdorf, H.; Satchi-Fainaro, R. Polymer therapeutics–polymers as drugs, drug and protein conjugates and gene delivery systems: past, present and future opportunities. *J. Drug Targeting* **2006**, *14*, 337−341.

(2) Shen, Y.; Jin, E.; Zhang, B.; Murphy, C. J.; Sui, M.; Zhao, J.; Wang, J.; Tang, J.; Fan, M.; et al. Prodrugs forming high drug loading multifunctional nanocapsules for intracellular cancer drug delivery. *J. Am. Chem. Soc.* **2010**, *132*, 4259−4265.

(3) Kim, Y.-H.; Bae, Y. H.; Kim, S. W. pH/temperature-sensitive polymers for macromolecular drug loading and release. *J. Controlled Release* **1994**, *28*, 143−152.

(4) Pervaiz, M.; Oakley, P.; Sain, M. Extrusion of thermoplastic starch: effect of "green" and common polyethylene on the hydrophobicity characteristics. *Mater. Sci. Appl.* **2014**, *05*, 845.

(5) Holohan, C.; Van Schaeybroeck, S.; Longley, D. B.; Johnston, P. G. Cancer drug resistance: an evolving paradigm. *Nat. Rev. Cancer* **2013**, *13*, 714−726.

(6) Mura, S.; Nicolas, J.; Couvreur, P. Stimuli-responsive nanocarriers for drug delivery. *Nat. Mater.* **2013**, *12*, 991−1003.

(7) Duan, X.; Bai, T.; Du, J.; Kong, J. One-pot synthesis of glutathione-responsive amphiphilic drug self-delivery micelles of doxorubicin−disulfide−methoxy polyethylene glycol for tumor therapy. *J. Mater. Chem. B* **2018**, *6*, 39−43.

(8) Wu, Y.; Wang, X.; Chang, S.; Lu, W.; Liu, M.; Pang, X. β-Lapachone Induces NQO1- and Oxidative Stress-Dependent Hsp90 Cleavage and Inhibits Tumor Growth and Angiogenesis. *J. Pharmacol. Exp. Ther.* **2016**, *357*, 466−475.

(9) Huang, G.; Chen, H.; Dong, Y.; Luo, X.; Yu, H.; Moore, Z.; Bey, E. A.; Boothman, D. A.; Gao, J. Superparamagnetic iron oxide nanoparticles: amplifying ROS stress to improve anticancer drug efficacy. *Theranostics* **2013**, *3*, 116−126.

(10) Li, T.; Amari, T.; Semba, K.; Yamamoto, T.; Takeoka, S. Construction and evaluation of pH-sensitive immunoliposomes for enhanced delivery of anticancer drug to ErbB2 over-expressing breast cancer cells. *Nanomedicine* **2016**, *13*, 1219−1227.

(11) Johnson, R. P.; Jeong, Y. I.; Choi, E.; Chung, C. W.; Kang, D. H.; Oh, S. O.; Suh, H.; Kim, I. Biocompatible Poly (2-hydroxyethyl methacrylate)-b-poly(L-histidine) Hybrid Materials for pH-Sensitive Intracellular Anticancer Drug Delivery. *Adv. Funct. Mater.* **2012**, *22*, 1058−1068.

(12) Cui, K.; Li, G.; Wang, L.; Guo, W.; Pei, M. An ON/OFF Aptasensor for Detection of AFB1 Based on pH-sensitive Polymer and GO Composite. *J. Electrochem. Soc.* **2020**, *167*, No. 027508.

(13) Wei, X.; Luo, Q.; Sun, L.; Li, X.; Zhu, H.; Guan, P.; Wu, M.; Luo, K.; Gong, Q. Enzyme- and pH-Sensitive Branched Polymer-Doxorubicin Conjugate-Based Nanoscale Drug Delivery System for Cancer Therapy. *ACS Appl. Mater. Interfaces* **2016**, *8*, 11765−11778.

(14) He, F.; Li, S.; Vert, M.; Zhuo, R. Enzyme-catalyzed polymerization and degradation of copolymers prepared from ϵ-caprolactone and poly (ethylene glycol). *Polymer* **2003**, *44*, 5145−5151.

(15) Dixon, S. J.; Lemberg, K. M.; Lamprecht, M. R.; Skouta, R.; Zaitsev, E. M.; Gleason, C. E.; Patel, D. N.; Bauer, A. J.; Cantley, A. M.; Yang, W.; et al. Ferroptosis: an iron-dependent form of nonapoptotic cell death. *Cell* **2012**, *149*, 1060−1072.

(16) Qiu, F.; Wang, D.; Wang, R.; Huan, X.; Tong, G.; Zhu, Q.; Yan, D.; Zhu, X. Temperature-induced emission enhancement of star conjugated copolymers with poly(2-(dimethylamino)ethyl methacrylate) coronas for detection of bacteria. *Biomacromolecules* **2013**, *14*, 1678−1686.

(17) Nkazi, B. D.; Neuse, E. W.; Sadik, E. R.; Aderibigbe, B. A. Synthesis, Characterization, Kinetic Release Study and Evaluation of

Hydrazone Linker in Ferrocene Conjugates at Different pH Values. *J. Drug Delivery Sci. Technol.* **2013**, *23*, 537−545.
(18) Cao, Y.; Liu, M.; Cheng, J.; Yin, J.; Huang, C.; Cui, H.; Zhang, X.; Zhao, G. Acidity-Triggered Tumor-Targeted Nanosystem for Synergistic Therapy via a Cascade of ROS Generation and NO Release. *ACS Appl. Mater. Interfaces* **2020**, *12*, 28975−28984.
(19) Liu, T.; Liu, W.; Zhang, M.; Yu, W.; Gao, F.; Li, C.; Wang, S.-B.; Feng, J.; Zhang, X.-Z. Ferrous-Supply-Regeneration Nanoengineering for Cancer-Cell-Specific Ferroptosis in Combination with Imaging-Guided Photodynamic Therapy. *ACS Nano* **2018**, *12*, 12181−12192.
(20) Gao, M.; Deng, J.; Liu, F.; Fan, A.; Wang, Y.; Wu, H.; Ding, D.; Kong, D.; Wang, Z.; Peer, D.; Zhao, Y. Triggered ferroptotic polymer micelles for reversing multidrug resistance to chemotherapy. *Biomaterials* **2019**, *223*, No. 119486.
(21) Suk, J. S.; Xu, Q.; Kim, N.; Hanes, J.; M, L. PEGylation as a strategy for improving nanoparticle-based drug and gene delivery. *Adv. Drug Delivery Rev.* **2016**, *99*, 28−51.
(22) Deng, Y.; Liu, X.; Huang, Z.; Yu, B.; She, Z.; Tian, Q.; Cheng, X.; Fan, D.; Song, Y. Self-assembled micelles of novel amphiphilic copolymer cholesterol-coupled F68 containing cabazitaxel as a drug delivery system. *Int. J. Nanomed.* **2014**, *9*, 2307−2317.
(23) Tang, Y. J.; Chen, Y.; Zhu, H. J.; Zhang, A. M.; Wang, X. L.; Dong, L. Z.; Li, S. L.; Xu, Q.; Lan, Y.-Q. Solid-phase hot-pressing synthesis of POMOFs on carbon cloth and derived phosphides for all pH value hydrogen evolution. *J. Mater. Chem. A* **2018**, *6*, 21969−21977.
(24) Xu, M.; Zhang, C.; Wu, J.; Zhou, H.; Bai, R.; Shen, Z.; Deng, F.; Liu, Y.; Liu, J. PEG-detachable polymeric micelles self-assembled from amphiphilic copolymers for tumor-acidity-triggered drug delivery and controlled release. *ACS Appl. Mater. Interfaces* **2019**, *11*, 5701−5713.
(25) Aliabadi, H. M.; Mahmud, A.; Sharifabadi, A. D.; Lavasanifar, A. Micelles of methoxy poly(ethylene oxide)-b-poly(epsilon-caprolactone) as vehicles for the solubilization and controlled delivery of cyclosporine A. *J. Controlled Release* **2005**, *104*, 301−311.
(26) Jian, J.; Sui, B.; Gou, J.; Liu, J.; Tang, X.; Xu, H.; Zhang, Y.; Jin, X. PSMA Ligand conjugated PCL-PEG polymeric micelles targeted to prostate cancer cells. *PLoS One* **2014**, *9*, No. e112200.
(27) Fairley, N.; Hoang, B.; Allen, C. Morphological control of poly(ethylene glycol)-block-poly(ε-caprolactone) copolymer aggregates in aqueous solution. *Biomacromolecules* **2008**, *9*, 2283−2291.
(28) Soppimath, K. S.; Tan, C. W.; Yang, Y. Y. pH-Triggered Thermally Responsive Polymer Core-Shell Nanoparticles for Drug Delivery. *Adv. Mater.* **2005**, *17*, 318−323.
(29) Xu, B.; Yuan, J.; Ding, T.; Gao, Q. Amphiphilic biodegradable poly(ε-caprolactone)-poly(ethylene glycol)-poly(ε-caprolactone) triblock copolymers: synthesis, characterization and their use as drug carriers for folic acid. *Polym. Bull.* **2010**, *64*, 537−551.
(30) Xun, W.; Wang, H. Y.; Li, Z. Y.; Cheng, S. X.; Zhang, X. Z.; Zhuo, R. X. Self-assembled micelles of novel graft amphiphilic copolymers for drug controlled release. *Colloids Surf., B* **2011**, *85*, 86−91.
(31) Licciardi, M.; Giammona, G.; Du, J.; Armes, S. P.; Tang, Y.; Lewis, A. L. New folate-functionalized biocompatible block copolymer micelles as potential anti-cancer drug delivery systems. *Polymer* **2006**, *47*, 2946−2955.
(32) Sun, H.; Guo, B.; Ru, C.; Meng, F.; Liu, H.; Zhong, Z. Biodegradable micelles with sheddable poly(ethylene glycol) shells for triggered intracellular release of doxorubicin. *Biomaterials* **2009**, *30*, 6358−6366.
(33) Liu, Z.; Tang, Z.; Zhang, D.; Wu, J.; Si, X.; Shen, N.; Chen, X. A novel GSH responsive poly(alpha-lipoic acid) nanocarrier bonding with the honokiol-DMXAA conjugate for combination therapy. *Sci. China Mater.* **2020**, *63*, 307−315.
(34) Mao, J.; Li, Y.; Wu, T.; Yuan, C.; Zeng, B.; Xu, Y.; Dai, L. A Simple Dual-pH Responsive Prodrug-Based Polymeric Micelles for Drug Delivery. *ACS Appl. Mater. Interfaces* **2016**, *8*, 17109−17117.
(35) Xu, Y.; Wang, L.; Li, Y. K.; Wang, C. Q. Oxidation and pH responsive nanoparticles based on ferrocene-modified chitosan oligosaccharide for 5-fluorouracil delivery. *Carbohydr. Polym.* **2014**, *114*, 27−35.
(36) Zhang, C.; Di, X.; Yao, S.; Zhao, B.; Lin, J.; Li, J. Self-assembled micelles based on pH-sensitive PAE-g-MPEG-cholesterol block copolymer for anticancer drug delivery. *Int. J. Nanomed.* **2014**, *9*, 4923−4933.

https://doi.org/10.1021/acsomega.1c04330
ACS Omega 2021, 6, 28242−28253